Proceedings World Geothermal Congress 2000
Kyushu - Tohoku, Japan, May 28 - June 10, 2000

OVER 10 YEARS OF GEOLOGICAL INVESTIGATIONS WITHIN THE HDR SOULTZ PROJECT, FRANCE

Albert Genter[1], Hervé Traineau[2], Béatrice Ledésert[3], Bernard Bourgine[1] and Sylvie Gentier[1]
[1]BRGM, 3 avenue Claude Guillemin, BP 6009, F-45060 Orléans Cedex 2, France
[2]CFG, 3 avenue Claude Guillemin, BP 6429, F-45064, Orléans Cedex 2, France
[3]UFR Sciences de la Terre, Labo. Sédimentologie Géodynamique, Univ Lille 1, F-59655 Villeneuve d'Ascq Cedex, France

Key Words: geology, fracture, granite, alteration hydrothermal, HDR, Soultz

ABSTRACT

Several deep wells were drilled in the Rhine graben (Soultz, France) to evaluate the geothermal Hot Dry Rock potential of a deep fractured granite reservoir. Three main boreholes, which reached 2200, 3600 and 5100 m depth, intersected a crystalline basement overlain by 1400m of Cenozoic and Mesozoic sediments. Based on extensive geological database collected from 1987 to 1999, deep geology of the Soultz reservoir including hydrothermal alteration studies as well as an extensive fracture evaluation were characterised from core analysis, well-logging and borehole imagery interpretations. Conceptual models of hydrothermally altered and fractured zones are proposed. In order to build small-scale fracture distribution observed at Soultz from core data, simulation of 3D fracture network was done stochastically. At higher scale, several deterministic geometrical models were built by assuming fracture size in 3D. They showed that some potential connecting paths are outlined between the deep wells.

1. INTRODUCTION

The European Hot Dry Rock Programme, located at Soultz-sous-Forêts (France), uses the geothermal anomaly of the Rhine graben to create a deep underground heat exchanger and to produce geothermal energy extracted from fractured rocks (Baria et al., 1998). In this area of extensional tectonic regime, the crystalline rocks are not outcropping but are covered by about 1.4 km of Cenozoic and Mesozoic sediments.

After more than 10 years of activities at Soultz, two deep wells, GPK-1 and GPK-2 were drilled into the granitic basement to depths of 3600 and 5100 m respectively and a third well, EPS-1, was fully cored in the porphyritic granite to 2230m. The horizontal distance between the two deep wells is about 500 m (Figure 1). In order to stimulate the fracture system, several phases of hydraulic fracturing were performed (Gérard et al., 1997). Although the site is located within the Rhine graben, the wells were drilled into a local horst structure, striking N20E and bounded by regional normal faults (Figure 2). During the drillings, several natural permeable formations were detected in fractured zones producing fluids characterised by a high salinity content of about 100g/l (Aquilina et al., 1997). The stress regime was obtained using the hydrofracture stress measurement method (Klee and Rummel, 1993). The direction of the maximum horizontal stress deduced from borehole image logs is about N170E. Baria et al. (1998) suggested that by extrapolating the stress profile at great depth, fluid injection of saline brines on favourably oriented joints may be rather easy.

From the 7000 m length drilled into the Soultz granite, chip cutting samples, core samples, geophysical measurements and borehole image logs were acquired, analysed and interpreted in order to characterise the fracture network properties as well as the mineralogical composition of the paleozoic granite.

The recent deepening of GPK-2 from 3800 to 5100 m depth, shows that at great depth there are still some fractures with hydrothermal alteration. Below 4700 m, petrographic facies variations are observed (Figure 3) with the occurrences of fine-grained granite facies (Genter et al., 1999).

Based on this extensive geological database collected from 1987 to 1999, the deep geology of the Soultz reservoir including hydrothermal alteration studies and fracture network was evaluated in terms of conceptual multiscale fracture model to understand the possible fluid pathways. Schematically, we consider that the Soultz granite shows two main scales of fracturing: small-scale fractures and fracture zones.

2. SMALL-SCALE FRACTURE STUDY

2.1 Fracture Typology

At core scale, structural analysis of the EPS-1 data sets has defined several fracture types in granite: sub-horizontal joints, steeply dipping filled-joints, and steeply dipping filled-sealed shear-fractures. About 3060 fractures were collected, described and stored into a structural database (Genter and Traineau, 1996).

The *sub-horizontal joints* correspond to sheet- joints caused by unloading. They only occur at the top of the granite paleosurface. About 100 sub-horizontal joints were measured on core.

The *steeply dipping filled- joints* are minor fractures filled by hydrothermal products. About 2160 filled-joints were measured from core analysis. In granite rock mass, they are often interpreted in terms of primary joints related to the thermal contraction of the intrusion. These primary fractures are generally closely linked to pervasive alteration which corresponds spatially to a disseminated but wide alteration. These primary features were lately filled by hydrothermal products (calcite, chlorite). They correspond to mode 1 fractures. In terms of scale, the filled-joints population would correspond to metric to plurimetric scale.

After the crystallisation of the pluton, the Soultz granite undergone a series of successive tectonic episodes. As

indicated by striation marks and slickensides, a part of the filled-joints was reactivated into mode 2 shear-fractures. The most important tectonic event corresponds to the formation of the Rhine graben during Tertiary. About 800 *steeply dipping shear-fractures* were identified and they may exhibit slight to prominent wall- rock alteration including argillization. Some of the sealed- faults with a thick hydrothermal filling show a free residual aperture due to incomplete sealing. In terms of scale, the shear-fracture population would correspond to metric, decametric and hectometric scale.

Only 1% of the natural fractures collected on the cores show a significant free aperture corresponding to a partial filling of the fracture plane by hydrothermal products. This free aperture corresponds to the separation between the two surfaces of a given fracture. Geodic quartz filling fractures are the main hydrothermal filling associated with partially opened fractures. This void network within fracture visible at core scale is not geometrically connected. It means that these fractures are not necessarily hydraulically active. There was only one natural permeable fracture observed during drilling (outflow of brines) at 2170 m depth in EPS-1 well.

This fracture typology is valid for core sample only. Unfortunately, it has not been possible to distinguish the above fracture types from borehole imagery alone, and consequently, all the determined planar discontinuities have been called fractures.

2.2 Analysis of Core and Images Logs

A detailed comparison was made between the data collected on cores and those provided by different imaging techniques in terms of fracture density, fracture orientation and fracture spacing distributions (Genter et al., 1997b; Tenzer, 1995).

Attributes of several thousand fractures were collected from several high-resolution imaging techniques such as borehole televiewer (BHTV), ultrasonic borehole imager (UBI), formation microscanner (FMS), and formation microimager (FMI). For well EPS-1, the strike, dip, and spacing of 3060 fractures were recorded from the cores and compared to the 517 fractures (only) observed on the BHTV images over the same depth interval. For well GPK-1, the strike, dip, and spacing of 1380 fractures collected from the BHTV were compared to the results of the UBI, FMS, and FMI images. Finally, for well GPK-2, the strike, dip, and spacing of 1792 fractures were determined from the UBI images.

Fracture density

The fracture density results are presented as a cumulative number of fractures versus depth. The lower is the slope, the higher is the fracture density (Figure 4). The fractures in well EPS-1 interpreted from the core data (Figure 4) show a higher fracture density content (3.77 fractures/m on average): low-fracture intervals (1520 to 1620 m and 1910 to 2040 m with 0.7 to 1.3 fractures/m, respectively, on average) coexist with high-fracture intervals (1770 m to 1840 m with 4.0 fractures/m on average) and also with intense-fracture zones (1420 to 1460 m, 1620 to 1660 m, 2050 to 2080 m, and 2150 to 2180 m with 9.0 fractures/m on average). The intense-fracture zones correlate with fault zones that developed hydrothermal alteration, and low-fracture intervals correspond to massive unaltered granite.

In well GPK-1, the distribution of the cumulative number of fractures versus depth obtained in the granite from the different imageries is plotted on Figure 4. The curves show regular trajectories with a change in slope around 1950-2050 m. The FMS detected about 0.83 fractures/m down to 2000 m, and the FMI detected about 0.37 fractures/m, respectively. The FMI resolution being higher than the FMS resolution, the lower fracture density recorded by the FMI below 1950-2050 m depth cannot be assigned to the change in imaging tool. This is confirmed by the fact that the BHTV collected about 1.15 fractures/m above 2000 m depth and only 0.42 fractures/m below this depth, giving an overall average of 0.63 fractures/m as well as with UBI analysis in GPK-2 well.

Then, the evaluation of the fracture density with depth shows a concentration of fractures in some spatially limited depth intervals (clusters) and that the top of the crystalline basement (1400-2000 m) is more fractured than the lower part (2000-3800 m).

Fracture orientation

In the granite, the EPS-1 cores show the two major fracture sets trending N-S (N0° to N40° 80°W and N170° 70°E). Whatever the borehole techniques used for collecting fractures, the orientation of the fractures defined on the image logs within the well GPK-1 and GPK-2 are quite in agreement with the results obtained from core data: the major near-vertical fracture set trending NNW-SSE and NNE-SSW. The N170E principal fracture orientation is also the orientation of the maximum horizontal stress field (Baria et al., 1998).

Fracture spacing

At core scale the measured spacing along the length of borehole EPS-1 follows a power law between 0.04 m and 4.0 m, i.e. over two decades with a slope of -0.90 (Figure 5). The experimental values at the two ends of the distribution curve deviate from the power law because of (a) the effect of under-sampling for spacings of less than 0.04 m and (b) the size of the measurement support for the largest spacings. The maximum measured spacing is 64 m, although the extrapolated theoretical curve gives values of the order of 500 m. The fracture-spacing distributions of BHTV, UBI, FMI, and FMS fit a negative exponential law with data ranging between 1 cm and 40 m.

3. CHARACTERISATION OF HYDROTHERMALLY ALTERED AND FRACTURED ZONES

3.1 Fracture Zone Geometry

In these wells, the fractured and altered zones are nearly vertical and the dominating striking directions are oriented N-S (N 0E 75°W) or NE-SW (N 150E 80°E). At Soultz, their average true width is about 2 m, comprised between 0.1 and 28.5 m. But as these values were defined from heterogeneous data (core data, well-loggings, BHTV), their geometrical characterisation is not well constraint.

The three boreholes intersected approximately 100 fracture zones that were localised from oriented borehole wall imagery (Figure 6). The distribution of these fracture zones again forms irregularly distributed clusters. Their spacing distribution shows that they follow a power law between 20 and 300 m with a slope of -1.09. The extrapolated theoretical curve gives a maximum spacing of about 500 m, which is the same value calculated from small-scale fracture spacing distribution.

3.2 Internal Organisation of Fracture Zones

Core analysis showed that the natural fractures are organised into clusters within the granite defining highly fractured zones (Figure 4). Fracture density which is not homogeneously distributed within such zones, tends to increase in the inner part of the fractured zone and mimics the alteration gradient. These zones are characterised by a high shear-fracture content (mode 2). Examination of the EPS-1 and GPK-1 cores revealed a general spatial pattern. Fracture zones are organised with a core of intense fracturing in which breccia, microbreccia and oriented cataclasites developed, corresponding to successive stages of brittle deformation (Figure 7). The primary minerals (silicates) of the granite have been partly dissolved developing a peripheral wall-rock alteration halo. Then, silica-rich fluids precipitated quartz in the inner part of the fracture zone evidenced by the deposition of thicker veins. Surrounding the core is an intermediate zone in which fracturing is less intense. Cataclased granite is present in this zone and hydrothermal alteration is less intense than in the central part. Lastly, an outer zone is characterised by low fracture density but fairly intense argillization of the granite. This outer zone is considered as altered wallrock.

Primary quartz usually remains stable, except in the permeable level located around 2175 m depth in EPS-1 where it also suffered dissolution. Wall rock effects, which are well developed near the margins of zones of intense fracturing, gradually vanish over a few meters in the unaltered granite (protolith). Detailed petrographic studies have revealed the presence of tosudite (a regular dioctahedral chlorite and smectite mixed-layer lithium-bearing mineral) and of organic compounds within the producing zone in well EPS-1 (Ledésert et al., 1996). The organic matter has probably been transported through the fracture network from overlying sedimentary reservoirs. Within the massive granite, the pervasive hydrothermal alteration occurred and is characterised by chlorite, corrensite, calcite, hematite and epidote crystallisation.

Mercury porosity measurements were performed on both whole rock samples and separated plagioclase crystals in order to determine the part of the whole porosity due to altered plagioclases. The porosity of the fresh Soultz granite is less than 1%. Porosity values obtained on whole rock altered samples range between 1.7% and 25%. Those obtained on altered plagioclase crystals range from 20% to 27%. The fractured-altered samples (breccia, microbreccia) are quite often less porous than the hydrothermally altered facies. This surprising result could be easily explained if we consider that the macroscopic fractures developed into the breccia facies are systematically sealed by hydrothermal products (mainly silica). These secondary deposits plugged both the fracture and its surrounding altered matrix and then reduced the porosity values. Within altered facies, the dissolution processes developed into primary plagioclase and biotite are quite abundant. As macro-scaled fractures are less numerous than into the fractured facies, the secondary porosity is hardly obliterated by hydrothermal deposition and thus the porosity values are higher. This is illustrated on Figure 8, which shows that the highest values take place laterally and the lowest values are more or less concentrated into the inner part of the conceptual fractured zone.

4. GEOMETRICAL MODELLING OF FRACTURES

An attempt to simulate 3D small-scale fracture systems from 1D well data has been proposed (Genter et al., 1997a). We used the fracture datasets collected in well EPS-1 in the clastic formation overlaying the granite massive. The main difficulty in developing stochastic fracture models for reservoirs is that our knowledge of fractures is limited to cores and bore-wall images, which only provide 1D data. Well data are not sufficient to define 3D fracture systems, and cannot therefore be used alone to infer important parameters, such as fracture size and connectivity. The 3D conceptual model was simulated using an hierarchical probabilistic procedure, which combines (1) the fracture orientation, spacing and thickness distributions defined in well EPS-1, and (2) the length distribution normalised with the length/thickness relationships defined in outcrop. The visualisation of a part of the near-well 3D small-scale fracture model for well EPS-1 is plotted on Figure 9. The model was calibrated by visualising a 1D fictitious well drilled within the simulated 3D fracture system, and by comparing the fracture intersections to the real fracture intersections of well EPS-1. The clustering organisation of fractures was also reproduced within the model. Upscaling of the near-well fracture model consists in considering that the median cluster intersected by well EPS-1 represents a branch of a large-scale normal fault.

Although a lot of assumptions exist concerning the 3-D extension of the fractured zones, an attempt for building up a 3-D deterministic geometrical model of the fault network was done, in order to predict the connection paths between the HDR geothermal doublet at the scale of the reservoir. During drilling operations carried out at Soultz (Baria et al., 1996), about 20 present-day permeable fractures were identified at depth in the different wells. They are striking NNE-SSW to N-S in well GPK-2 and NW-SE, N-S and NE-SW in well GPK-1. This nearly-vertical permeable network was modelled geometrically (Figure 10) and shows that some connecting paths occur between well GPK-1 and Well GPK-2.

5. CONCLUSION

After 10 years of geological investigations at Soultz based on deep drilling reconnaissance, new ideas of the deep geology were outlined mainly in terms of geological model of hydrothermally altered and fractured granite reservoir. Such a conceptual model is mainly controlled by the structural tectonic history of this area, e.g. young graben formation. During forced-fluid circulation experiments, injected fluids will probably circulate through an altered porous and fractured rockmass composed of clays and secondary quartz than an unaltered granite. For a better understanding of the deep fractured reservoir at Soultz, we have therefore to consider the 3D multiscale structure of fractures.

ACKNOWLEDGEMENTS

This research was carried out in the framework of the European Hot Dry Rock Project, funded by the European Commission. Geological investigations were supported by the Research Division of BRGM. The authors are grateful to Dr. S. Bellani from ENEL and to an anonymous reviewer for the review of this paper.

REFERENCES

Aquilina, L., Pauwels, H., Genter, A., and Fouillac C. (1997). Water-rock interaction processes in the Triassic sandstone and the granitic basement of the Rhine graben : geochemical investigation of a geothermal reservoir. *Geo. et Cosmo. Acta* 61-20, pp.4281-4295.

Baria, R., Baumgärtner, J., and Gérard, A. 1996. *European Hot Dry Rock programme 1992-1995*. Edited by R. Baria, J. Baumgärtner & A. Gérard, Contract JOU2-CT92-0115, 328pp.

Baria, R., Baumgärtner, J., Gérard, A., and Jung, R. (1998). *European Hot Dry Rock geothermal research programme 1996-1997*. Contract N°: JOR3-CT95-0054, Joule III Programme, final report EUR 18925 EN, 151pp.

Genter, A., Castaing, C., Bourgine, B., and Chilès JP. (1997a). An attempt to simulate fracture systems from well data in reservoirs, ISRM International Symposium, NYRocks'97, *36th U.S. Rock Mechanics Symposium*, June 29-July 2, 1997, Columbia University, New York, USA, *Int. J. Rock Mech. & Min. Sci.* 34:3-4, paper No. 044.

Genter, A., Castaing, C., Dezayes, C., Tenzer, H., Traineau, H., and Villemin, T. (1997b). Comparative analysis of direct (core) and indirect (borehole imaging tools) collection of fracture data in the Hot Dry Rock Soultz reservoir (France). *J. of Geoph. Res.*, Vol 102, B7, pp.15419-15431.

Genter, A., and Traineau, H. (1996). Analysis of macroscopic fractures in granite in the HDR geothermal EPS-1 well, Soultz-sous-Forêts (France), *J. Volcano. Geotherm. Res.,* 72, pp.121-141.

Genter, A., Homeier, G., Chevremont, Ph., Tenzer, H. (1999) Deepening of GPK-2 HDR borehole, 3880-5090 m, (Soultz-sous-Forêts, France). Geological monitoring. *BRGM Open File Report R 40685*, 44 pp.

Gérard, A., Baumgärtner, J., and Baria, R. (1997). An attempt towards a conceptual model derived from 1993-1996 hydraulic operations at Soultz, *NEDO International Geothermal Symposium*, vol. 2, pp.329-341.

Klee, G., Rummel, F. (1993). Hydrofrac stress data for the European HDR research test site Soultz-sous-Forêts, *Int. J. Rock Mech. Min. Sci. & Geomech. Abstr.*, vol. 30, n°7, pp.973-976.

Ledésert, B., Joffre, J., Amblès, A., Sardini, P., Genter, A., and Meunier, A. (1996). Organic compounds: natural tracers of fluids circulations between sediments and the granitic basement at Soultz-sous-Forêts (France), *J. Volcano. Geotherm. Res.*, 70 (3-4), pp.235-253.

Tenzer, H. (1995). Fracture mapping and determination of horizontal stress field by borehole measurements in HDR drillholes Soultz and Urach, *World Geothermal Congress, 18-31th May 1995, Florence, Italy*, pp.2649-2655.

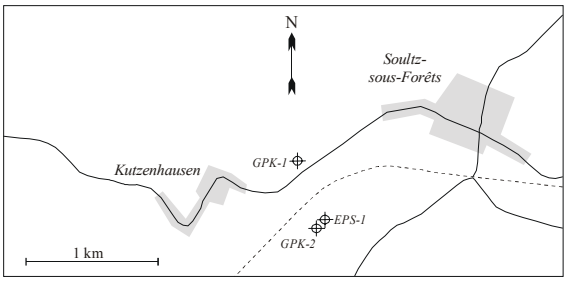

Figure 1. Location of the HDR borehole network at Soultz.

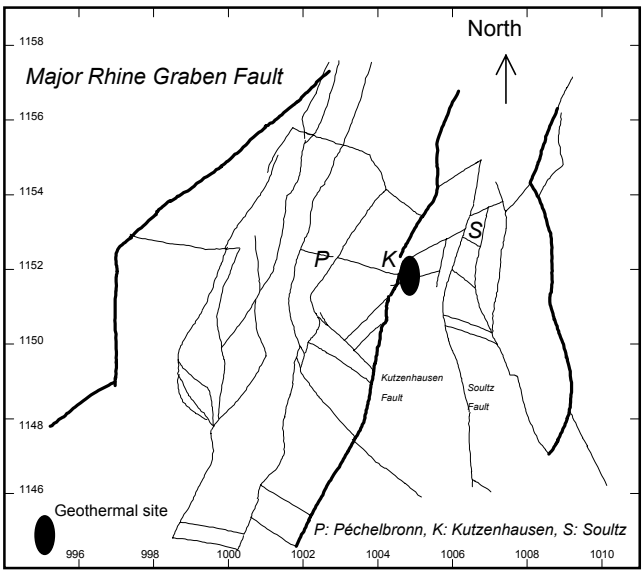

Figure 2. Schematic structural map around the Soultz site. The major normal faults are underlined in bold

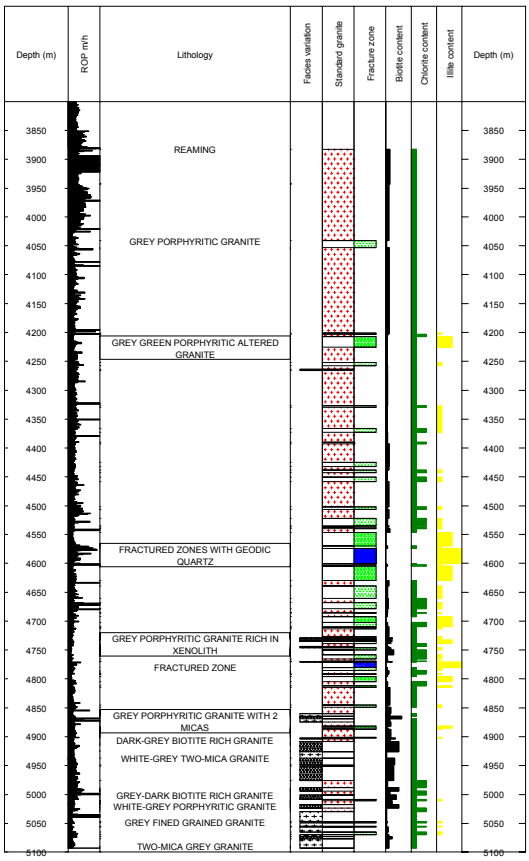

Figure 3. Geological profile of the deepest well at Soultz from 3900 to 5100 m depth

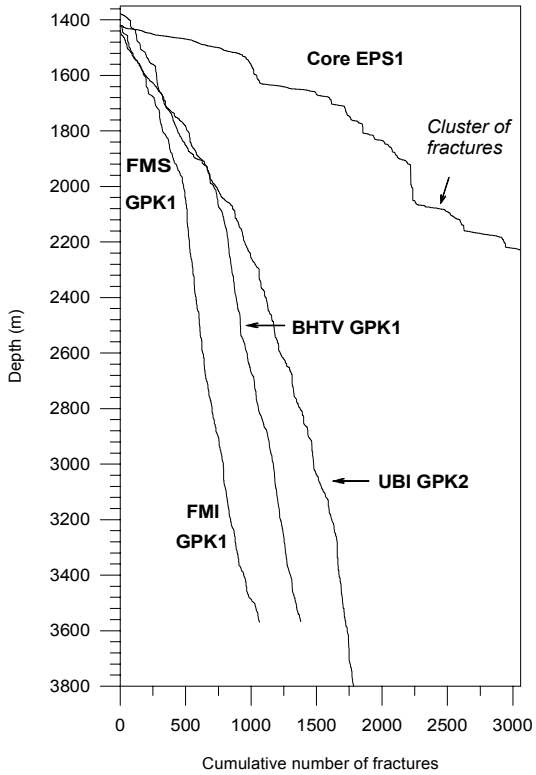

Figure 4. Cumulative number of fractures versus depth for fractures collected in wells GPK-1, GPK-2 and EPS-1

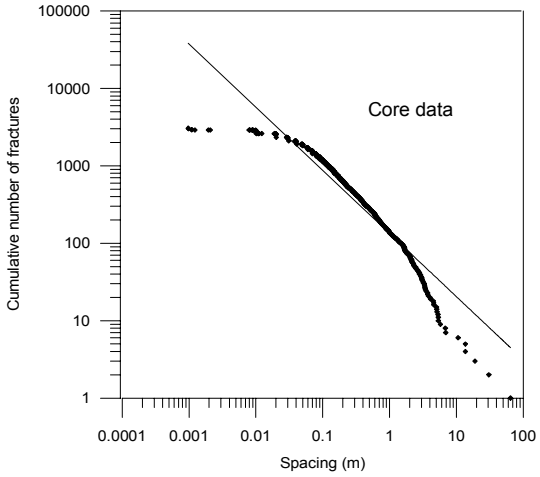

Figure 5. Cumulative distribution of fracture spacing from core analysis in granite of well EPS-1

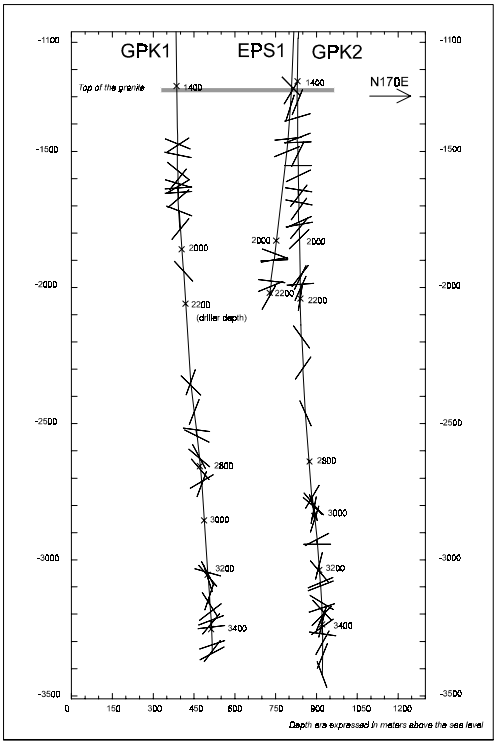

Figure 6. Vertical cross-section oriented N170°E showing the location of fractured zones intersecting the wells

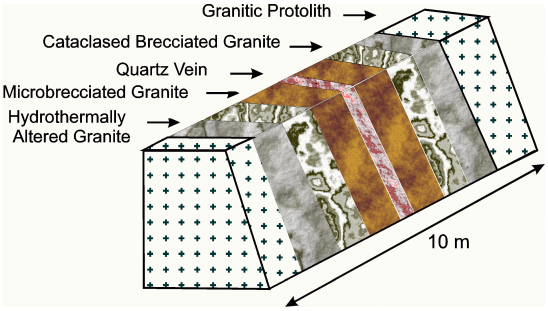

Figure 7. Conceptual lithofacies granite zonation of hydrothermally altered and fractured zone

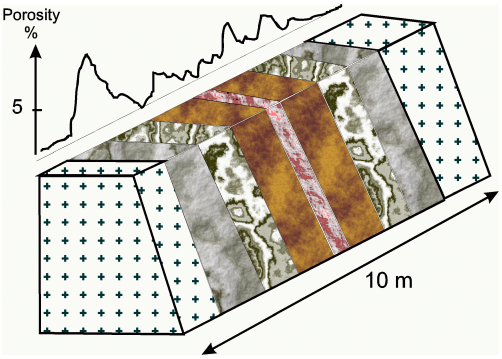

Figure 8. Porosity profile in a conceptual lithofacies granite zonation of hydrothermally altered and fractured

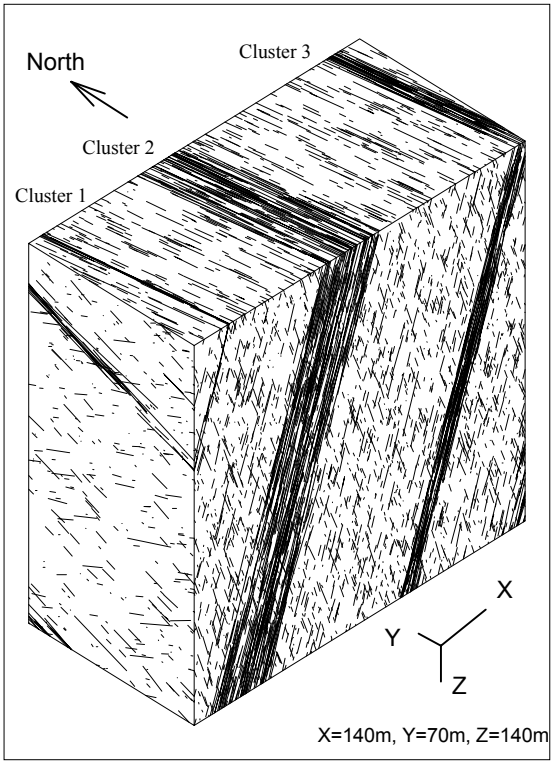

Figure 9. Visualisation of a part of the near-well 3D fracture model for well EPS-1 (from Genter et al., 1997a)

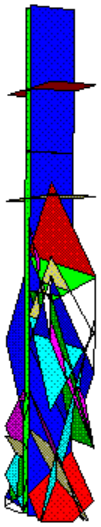

Figure 10. Geometrical modelling of fractured permeable zones in the Soultz granite along a N170E oriented cross-section between wells GPK-1 and GPK-2. The horizontal features represent the major sedimentary formations